Available online at www.sciencedirect.com
SCIENCE DIRECT
Sensors and Actuators B 113 (2006) 398–409
SENSORS AND ACTUATORS B CHEMICAL
www.elsevier.com/locate/snb

Small volume PCR in PDMS biochips with integrated fluid control and vapour barrier

A. Ranjit Prakash [a], S. Adamia [b,c], V. Sieben [a], P. Pilarski [a], L.M. Pilarski [b,c], C.J. Backhouse [a,*]

[a] *Department of Electrical and Computer Engineering, 2nd Floor, Electrical and Computer Engineering Research Faculty (ECERF), University of Alberta, Edmonton, Alta., Canada T6G2V4*
[b] *Department of Oncology, University of Alberta, Edmonton, Alta., Canada*
[c] *Cross Cancer Institute, Edmonton, Alta., Canada*

Received 29 July 2004; accepted 18 March 2005
Available online 28 April 2005

Abstract

In this paper we demonstrate a new method for microfabricating PDMS devices that controls vapour diffusion, thereby reducing water loss at elevated temperatures and greatly increasing the reliability of the PCR. In the past, the vapour and liquid diffusion properties of the PDMS material in microfluidic devices have impaired performance. We show that this water loss is primarily due to vapour diffusion from the PDMS biochip and by implanting a polyethylene vapour barrier layer in the PDMS, the overall fluid loss was almost eliminated (reduced by a factor of 3). We have also developed a procedure to ensure irreversible bonding between the PDMS and the implant. With this improved microfabrication method we demonstrate the feasibility and advantages of performing small volume PCR genetic amplification (i.e. with less than 2 μl of PCR sample) within a PDMS–glass hybrid biochip. Diaphragm pumps and pinch-off valves were integrated in the system and these enabled fluid retention during the amplification stage and will facilitate higher levels of on-chip automation.

Keywords: PDMS; PCR; Microfluidic; Diffusion; Micropump and microvalve

1. Introduction

Genetic analysis has become indispensable in a wide range of applications. In recent years the development of methods based on micromachining and biomedical microelectromechanical systems (bioMEMS) has provided an opportunity for performing bioassays in a novel, inexpensive, portable, and integrated manner in microfluidic devices (also known as biochips) [1–3]. The potential of research in this field is to make DNA testing a part of everyday life without the assistance of expensive laboratories. As the microfluidic biochip technology evolves, bioMEMS might greatly improve the accessibility of medical diagnostics.

The polymerase chain reaction (PCR) [4,5] is an enzymatic genetic amplification technique for the exponential replication of DNA molecules and is a key component of many methods for performing genetic analysis. Biochip PCR gives low reagent consumption and faster processing while allowing the production of highly integrated devices for high-throughput multiplexed diagnostic applications [5]. Glass and Si have been extensively used in the microfabrication of these devices [5] and the PCR has been successfully demonstrated in these materials with nanoliter [6] and even picoliter volumes [7]. More recently, many research groups have explored alternative materials for fabricating PCR devices and these include polycarbonate [8], polyimide [9], epoxies [10] and polydimethysiloxane (PDMS) [11].

PDMS, an inexpensive elastomeric polymer, has emerged as a promising material for bioMEMS applications [12]. The soft-lithography replica moulding of PDMS devices is revolutionizing microfluidic application as it facilitates rapid prototyping with features size as small as 2 nm [13]. Among the silicone rubber polymers, PDMS exhibits the

* Corresponding author. Tel.: +1 780 492 2920; fax: +1 780 492 1811.
E-mail address: chrisb@ualberta.ca (C.J. Backhouse).

0925-4005/$ – see front matter © 2005 Elsevier B.V. All rights reserved.
doi:10.1016/j.snb.2005.03.049

Table 1
Summary of physical/chemical properties of PDMS

PDMS property	Value
Chemical structure (repeating groups) [15,16]	O—Si$(CH_3)_2$
Shear modulus (high elasticity) [17]	100 kPa to 3 MPa
Density [50]	920 kg/m^3
Surface tension of wetting [15]	23 mN/m
Water contact angle (virgin—hydrophobic) [15,16]	>100°
Glass transition temperature (low) [15]	−127 °C
Thermal conductivity (low) [23]	0.17 W/m K
Permeability to water (high for polymers) [35]	80.5×10^{-11} g cm/cm^2 s cmHg
Diffusion coefficient of water [22]	$\sim 2 \times 10^{-9}$ m^2/s
Water uptake capacity (high for polymers) [46]	0.38% (w/w)
Activation energy for water diffusion [22]	14 kJ/mol

highest flexibility [14]—a result of its low glass transition temperature, high free volume and porosity [15–17] (see Table 1). The flexibility of the PDMS is also advantageous in that it enables simple microfluidic valving and pumping techniques [18–20]. However, the properties of PDMS that give it its flexibility (e.g. high free volume) are also responsible for its very significant vapour and liquid diffusion properties [21,22]. While these diffusion properties have been advantageously used in membrane applications for the vapour separation of volatile gases [21], they are undesirable in many microfluidic devices as they can result in the rapid loss of reagents through vapour loss (especially loss during the thermal cycling used in the PCR process) [23]. The resulting vapour loss changes the concentrations of the PCR reagents (sometimes leading to a complete drying-out) [23] and this is often the cause of unsuccessful genetic amplification.

There have been relatively few reports of PCR performed in PDMS devices [11,23–26] and each of these reports appears to have developed means of coping with this liquid loss, often through the simple expedient of using large liquid volumes. The early demonstration by Fujii and coworkers [11] used sample volumes as high as 50 μl. This was an important step in developing PDMS-based on-chip PCR but such large volumes are comparable to those of conventional methods, thereby losing many of the advantages of miniaturization. Although Liu et al. [26] and Yu et al. [24] subsequently showed successful results with arrays of small volume PCR wells, we attribute their success to the use of a particular chip geometry that may not be suitable for other integrated chip designs. More recently, Shin et al. [23] performed small volume PCR (∼2 μl) in PDMS devices and explicitly addressed the sample loss problem by surface coating the PDMS with a vapour barrier of Parylene C. The Parylene coating may impede irreversible PDMS bonding and we know of no reports of bonding Parylene in a MEMS device and in fact, Parylene C is used as a ‘release agent’ in MEMS processing [10]. The Parylene surface coating was applied by a chemical vapour deposition method that used a dedicated off-site deposition system in another facility. Such a surface coating can significantly increase fabrication costs and can greatly hinder the use of PDMS as a rapid prototyping material.

The water diffusion/vapour loss property of PDMS has been a concern in other microfluidic applications and is an issue that has only recently been addressed in the literature. Chang et al. [28] reported of fluid loss in PDMS microfluidic devices during bacterial culture. In order to minimize this loss, the proportion of the curing agent to the PDMS pre-polymer was varied to fabricate their PDMS devices. However, increasing the proportion of the curing agent to the pre-polymer results in rigid PDMS structures that are incompatible with PDMS-based pumping and valving techniques [18,20,29].

In the present work, we demonstrate the severity of the vapour loss problem and present an easily implemented method to minimize this loss. We show that the vapour loss can lead to the failure of the PCR and show that the vapour diffusion from PDMS microfluidic devices during thermal cycling can be reduced several-fold by implanting a polyethylene (PE) vapour barrier in the PDMS. A protocol to obtain irreversible bonding between the implant and the PDMS was also developed. Since the implanted vapour barrier is inside the PDMS and does not make any contact with the PCR reaction mix, issues concerning the inhibition of genetic amplification by the implanted material do not arise.

Sylgard 184 PDMS (Dow Corning) has been demonstrated to be an effective material for fabricating microfluidic devices. However, to the best of our knowledge, no diffusion studies in this PDMS have been reported [28]. Here we investigate two diffusion-based mechanisms for the loss of liquid from PDMS devices—vapour loss from the PCR chamber to the atmosphere and absorption of the liquid by the PDMS bulk. Our results indicate that the vapour loss is the dominant factor.

In this work we have also integrated fluid control in our biochip using diaphragm pumping [18] and pinch-off valving techniques [20,29]. The valves and pump were operated in an automated fashion by servomotor actuators and provided a fully reusable microfluidic valving and pumping system—an important step in the ongoing development of highly integrated systems.

2. Materials and methods

2.1. Biochip fabrication

The PDMS–glass hybrid biochip design is depicted in Fig. 1, consisting of two open exterior reservoirs interconnected by microchannels to an enclosed PCR chamber at the centre. We patterned these microchannels, ports, reaction chambers, and reservoirs in PDMS using the soft-lithography approach [27] and bonded the PDMS to a glass substrate. The PDMS overlayer was a three-layer structure in which the top and bottom layers were composed of PDMS while the middle layer was a PE implant embedded in the PDMS. The PDMS structure was then sealed to a glass substrate to produce a hybrid biochip (22 mm × 11 mm × 3 mm) with enclosed microchannels (10 mm × 20 μm × 50 μm) and a PCR chamber (1.75 μl).

Chip designs were drawn in L-Edit v3.0 (MEMS Pro 8, MEMS CAP, CA, USA) and then transferred to a chromium mask wafer using a pattern generator (DWL 200, Heidelberg Instruments, CA, USA). This mask was then used to prepare a master mould for PDMS casting, the master consisting of a thick patterned photoresist layer atop a glass substrate. The process to prepare this master pattern was as follows: A 4 in. × 4 in. Borofloat glass substrate (Paragon Optical Company, PA, USA) was first cleaned in a fresh Piranaha solution (1:3 by volume of hydrogen peroxide and sulphuric acid), rinsed with deionized water in a spin-rinse-dryer and dried with a nitrogen pressure gun. To ensure good adhesion of the photoresist, a chromium adhesion layer was then applied to the glass. The glass substrate was sputter coated with a layer of chromium to a thickness of ∼200 nm (pressure with argon gas = 7 mTorr and power = 300 W) in a sputtering system (KJLC-CMS-18HV, Kurt J Lesker, Clariton, USA). The metallized glass substrate was then spin-coated (model # 5110-CD, Solitec Spinner, CA, USA) with SRJ5740 ultra-thick photoresist (Shipley Microelectronics, MA, USA) at a spin speed of 200 rpm for 10 s and a spread speed of 1500 rpm for 15 s, and then soft-baked in an oven at 115 °C for 60 min. The substrate was then stored overnight in a light-tight container with a beaker of water (10 ml) before further processing. (Overnight-humidified storage of the SRJ5740 photoresist was found to quicken the chemical developing process after UV exposure.) UV exposure (30 s, 356 nm, intensity of 19.2 mW/cm^2) of the spin-coated substrate was performed through the chrome mask using a mask aligner system (ABM Inc., CA, USA). The substrate was then chemically developed with Developer 354 (Shipley Microelectronics, MA, USA) for about 45 min—end time determined by visible inspection. The patterned photoresist then served as a master mould for the PDMS replica moulding [27] and it was typically reused many times. The features of the photoresist were inspected on an optical profilometer (model # 99-33-50083, Zygo Corp., CT, USA). A single coating of this photoresist gave a channel height of 18 μm (with a 10% variation between coated wafers). Posts made of stainless steel with radii of ∼0.75 mm and heights of 1 mm were cleaned by a brief immersion in Piranha, rinsed, dried and placed upon the master mould at the locations for the PCR chambers. The PDMS did not adhere to the posts, and there was no significant seepage of PDMS underneath the posts. The pre-polymer of PDMS and the curing agent (Sylgard 184, Dow Corning, NC, USA) totalling 20 g were mixed in proportions of 1:10, stirred mechanically and degassed in a vacuum chamber (model # 1415M, Shelldon Lab, OR, USA) at 20 in.Hg for 20 min prior to use. A PE layer was sandwiched within two PDMS layers by either the chemical or physical method described below.

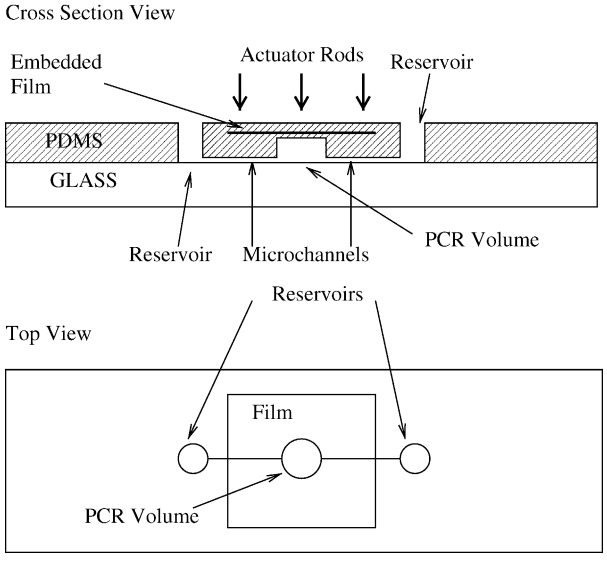

Fig. 1. Diaphragm pump and pinch-off valve in a PDMS–glass hybrid chip.

2.1.1. Chemically implanted method

PE film (Glad Metric Offer, Ont., Canada) is easily soluble in hydrocarbon solvents like toluene and xylene [30]. We chose toluene (Fair Lawn, NJ, USA) as a solvent to dissolve the PE due to its moderate interaction and absorption by the PDMS [31] as this causes an inter-diffusion of the dissolved PE into the PDMS structure and results in an irreversible interfacial adhesion between the implanted PE and the PDMS. PE (0.5 g) and toluene (25 ml) were placed in an Erlenmeyer flask with a magnetic stir bar in the flask. The Erlenmeyer flask was then mounted on a stirrer-hot plate instrument (Isotemp, Fisher Scientific, Ont., Canada) and stir-heated at 200 rpm and 110 °C. After 10 min of stir-heating, the PE was completely dissolved and a homogeneous liquid mixture was obtained. (*Caution:* Toluene is a carcinogenic, aromatic hydrocarbon and care should be taken for safe handling inside a fume hood. The Erlenmeyer flask should remain uncapped at all times to prevent pressure build-up in the flask.) To implant the PE, first a portion of the liquid PDMS (15 g) was poured into the holder housing the master. Then the homogenous mixture of toluene and PE was poured over the PDMS and left to dry for about 15 min (causing visible drying of the toluene). The thickness of the PE implant layer

is ∼35 μm on the 4.2 in. × 4.2 in. wafer mould assuming a distinct layer and a 25% handling loss (since some residues were left behind in the flask). To increase the thickness of the PE layer, more dissolved PE could be used or the layering process can be repeated. After the partial drying of the toluene, the remaining portion of the PDMS (5 g) was poured on the master, making up a total thickness of about 2 mm.

2.1.2. Physically implanted method

In this method a pre-cast PE film of 12.7 μm thickness (Glad Metric Offer, Ont., Canada) was used. The process was similar to the chemical implant method in that 15 g of the PDMS was poured in a holder housing the master. The PE film was then introduced on the surface of the PDMS before the remaining PDMS (5 g) was poured on the master; thus creating a weakly bonded implant of the PE film.

2.1.3. Curing for either method

The PDMS with the implanted PE was thermally cured in an oven at 90 °C for 1.5 h and then the temperature was ramped (approx. at the rate of 1 °C/min) and held at 135 °C for 10 min. This elevated temperature softened the PE implant near its melting point (137 °C) for better adhesion of the PE to the PDMS. This elevated temperature step was required for irreversible adhesion of the PE to the PDMS for the physical implant method (as discussed in Section 4.2) but was not essential for the chemical implant method (where irreversible adhesion was achieved, likely due to inter-diffusion of the PE in the PDMS).

The cured PDMS (with the implanted PE) was peeled-off from the master, the posts removed, and the PDMS was diced along chip boundaries with a razor blade. Glass substrates were diced in a dicing-saw, Piranaha-cleaned to remove any organic surface contaminants, rinsed in deionized water, and finally dried in nitrogen to render the glass surface hydrophilic. The PDMS was then bonded to the cleaned glass using a protocol in which an oxygen plasma and hot-plate treatment gives an irreversible bond. This protocol is similar to that described by the Whitesides group [31]. The mating surfaces of the PDMS and glass were placed face-up in a reactive ion etch (RIE) (Plasmalab, Plasma Technology, Bristol, UK), with 80% O_2 gas flow at a chamber pressure of 0.15 Torr, a power of 35 W and treated for 70 s. After the plasma treatment and the venting of the RIE system (venting takes about 2 min), the PDMS and glass were removed from the system and the mating surfaces were then brought into contact immediately (within 1 min of being removed from the system). A mild pressure was then applied, followed by a thermal treatment on a hot plate for 5 min at 100 °C. Care was taken to prevent contact of any material on the mating surfaces of the PDMS or the glass prior to bonding as it prevented irreversible bonding of the surfaces in those areas. Pre-treatment of the RIE was required and this involved manually cleaning the floor of the chamber with a clean-room wipe (ideally moistened with isopropanol) and a 'dummy-run' for 30 min with the same parameters as the bonding protocol. In the final stage, reservoir holes to access the channels are punched with a custom-made hand-punch. 'Scotch-tape' adhesion strength tests of the implant in the PDMS and the bonding were performed by affixing an adhesive tape (Scotch Tape, 3M Chemicals, Ont., Canada) to the device and peeling the tape away.

2.2. Microfluidic pumping and valving

The concept of diaphragm pumping in MEMS was introduced by Stemme and coworkers with polycarbonate and Si structures [32]. The use of PDMS has highly simplified the design [18] due to its very high flexibility with negligible variation in shear modulus even at +100 °C (1.1 kPa/°C) [14,15]. These PDMS properties are useful in implementing diaphragm pumping and pinch-off valving techniques and are suited for stable operation within the PCR thermal cycling temperature range (50–94 °C).

In our hybrid PDMS–glass biochip the enclosed PCR chamber has a 1 mm thick PDMS roof structure that also serves as the diaphragm pump. This simplifies the chip design, increases the device density and reduces the fluid dead volume in the chip. The pinch-off valving [29] of the channels is achieved by sealing the PDMS against the lower rigid glass substrate by external actuators as described below; the working principle is similar to that of the NanoFlex™ valve [20].

Fig. 1 is a schematic of the diaphragm pump and pinch-off valves for our chip. The downward and upward movements of rods above the surface of the PDMS are controlled by servo-motors to perform the steps of channel sealing, fluid loading and unloading. We have found that it is very important to seal-off the PCR chamber during the thermal cycling of the PCR process. Since the actuating rods are not in direct contact with the fluid sample, inhibition and cross-contamination issues do not arise. This simple yet effective concept of diaphragm pump and pinch-off valves provides a compact and reusable fluid control system suitable for PCR genetic amplification and a wide variety of other microfluidic applications.

2.3. PCR experimentation

As PCR volumes are decreased in biochips, genetic amplification is increasingly prone to biochemical surface absorption problems at the chamber walls due to the increasing surface area-to-volume ratio [33]. Bovine serum albumin (BSA) and polyethylene glycol (PEG) are commonly used to counteract this absorption phenomenon [5]. Prior to loading the PCR reaction mix, the PCR chamber and the channels were pre-treated for 30 min by filling them with a solution of 10 mg/ml of BSA (diluted in doubly distilled water (DDW)). The PCR product was amplified from yeast genomic DNA with 24 base primers specific to the SCO1 gene. The primer sequences were 5′-GACTGCTAGGAATTCAGCAATGGC-3′ (forward) and 5′-ATATAATCGGCATGCGAAACGTATG-3′ (reverse). The

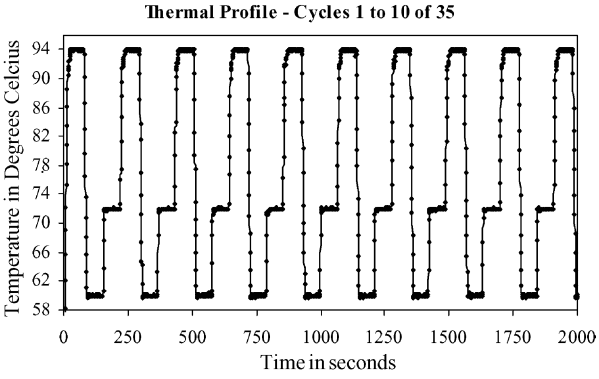

Fig. 2. Thermal cycling profile of the custom-built on-chip PCR thermal cycler controlled by an in-house 'non-linear digital PD-PI controller'.

primers were purchased from Synthetic Genetics (San Diego, CA, USA) and both were labelled with the fluorophore Cy5. Further details on PCR performed with this gene can be found elsewhere [34]. A PCR reaction master mix of 25 μl was prepared of which ∼1.75 μl was loaded in a PCR biochip and the remainder was used for a control run on a commercial thermocycler (PTE-200, MJ Research, MA, USA). The protocol for the PCR reaction master mix was as follows, 2 μl of each primer (1 pmol/μl), 1.6 μl of yeast nDNA (150 ng), 2 μl of dNTPs (2.5 mM), 2.5 μl of 10× PCR buffer (Tris–HCl 200 mM (pH 8.5), KCl 500 mM), 2.5 μl of BSA diluted in DDW (1 mg/ml), 0.75 μl of $MgCl_2$ (1.5 mM), 0.5 μl of Taq polymerase, and 11.1 μl of DDW.

The thermal cycling consisted of an initial denaturation at 94 °C for 2 min followed by 35 cycles of denaturation (94 °C), annealing (55 °C) and extension (72 °C) for 60 s each with a final extension (72 °C) for 10 min. Thermal cycling for on-chip PCR (with both modified and unmodified chips) was performed in a custom-built Peltier device controlled by an in-house 'non-linear digital PD-PI controller' with programmable gain constants. Efficient temperature transitions (up to 4.5 °C/s) and a steady-state stability of less than ±0.1 °C were achieved with accurate gain-constant tuning and the thermal response (Fig. 2) was typical of a critically damped system. The system performance is comparable to, if not better than, most commercial thermocyclers used for conventional tube PCR.

2.4. Diffusion loss experiments

PDMS exhibits high volatile gas/vapour permeability [21] and especially very high water/water vapour permeability (Table 2) [35]. To quantify the sample loss resulting from the diffusion properties of the PDMS during the PCR thermal cycling we performed experiments in which PDMS biochips were loaded with DDW samples and subjected to thermal cycling (94, 60 and 72 °C for 30 s each). After a predefined number of thermal cycles, the sample from the chip was unloaded and quantified in a micropipette (Pipetman, Gilson, WI, USA). The micropipette quantification was done by first setting the micropipette to 2.25 μl (25% above known maximum fluid volume) and then with the micropipette depressed (expulsion mode), the micropipette tip was immersed into the liquid. This was followed by collecting the liquid into the micropipette tip (suction mode) and since the micropipette was set to a quantity slightly more than was initially loaded, the liquid was completely collected and was followed by as much as 0.5 μl of air. By adjusting the setting on the micropipette until the air is again expelled, the amount of remaining liquid can be determined. Albeit crude, this method avoids handling and evaporation losses and with numerous tests of known quantity of liquid we have found our uncertainties to be ±5% (consistent with the specifications for this device as provided by the manufacturer).

Measurements were made after 0, 5, 10, 20, and 35 cycles and a progressive loss was found with increasing cycle number. We refer to the graphical representation of this fluid loss as a 'diffusion curve'. Four such diffusion curves were obtained from separate experiments. The first diffusion curve experiment was performed in a PDMS chip without a vapour barrier implant. The second was performed in a PDMS chip with a smooth, flat glass piece (or capping, 3 mm × 3 mm × 1 mm) pressed against the PCR chamber. The glass capping was held firmly against the PDMS surface by rod 2 of our pumping system (Fig. 1) and was seen to make intimate contact (i.e. no air gap) with the flat top surface of the PDMS. The third and the fourth diffusion curve experiments were performed in PDMS chips that were fabricated with a PE vapour barrier implant (using each of the implantation methods described above).

Table 2
A list of low water permeability polymers as potential implant materials in PDMS to prevent vapour diffusion

Material	Water/water vapour permeability [35] ($\times 10^{-11}$ g cm/cm^2 s cmHg)	Suggested solvent[a] [30]	Swelling ratio (S) of solvent in PDMS[b] [31]
PDMS	80.5	–	–
Poly(vinylidene chloride)	∼0.052	Cyclohexane	1.33
Polypropylene	0.42	Trichloroethylene	1.34
Polyethylene (LDPE)	0.83	Toluene	1.31
Polyacrylonitrile	2.45	Dimethylformamide	1.02
Poly(vinyl chloride)	2.5	Xylene	1.41
Fluoropolymers (3M, Canada)	N/A	Acetone	1.06

[a] Heat may be required for dissolution.
[b] $S = D/D_0$, where D is the length of the PDMS in the solvent and D_0 is the length of the dry PDMS. S values are based on the experimental data on a cured PDMS sample [31].

2.5. Capillary electrophoresis

The retrieved PCR product was analysed on a cross channel capillary electrophoresis (CE) chip (Micralyne, Edmonton, Canada) in which the sample and sample waste, and buffer and buffer waste wells are connected by two intersecting channels. The Microfluidic Tool Kit (Micralyne, Edmonton, Canada) provides the high voltage to separate the primers from the product DNA in the CE chip. A laser induced fluorescence (LIF) detection system provided excitation at a wavelength of 635 nm and detection at 670 nm. The system was controlled by a LabVIEW control program supplied by Micralyne.

The channels in the chip were loaded with a sieving medium (GeneScan polymer, Applied Biosystems, Foster City, CA) by syringe. The sample waste, buffer, and buffer waste wells were filled with 3 μl of 1× TBE running buffer. The on-chip PCR product was diluted in 0.1× TBE to constitute a total volume of 3 μl and loaded in the sample well. In the case of the control experiment product analysis, only 0.3 μl of the PCR product was used and this was then diluted with 2.7 μl of 0.1× TBE and loaded in the sample well. An injection voltage of 0.4 kV was applied for 60 s between the sample and sample waste well to move the PCR product from the sample well to the channel intersection. This was followed by a separation voltage of 6 kV applied between the buffer and buffer waste well, and this resulted in the transport of the DNA caught in the intersection towards the buffer waste well. During this transport, the primer and product DNA move with different velocities and their arrival was detected at a distance of 76 mm from the channel intersection. More detail can be found in prior work [34,36].

3. Results

3.1. Diffusion loss experiment analysis

Fig. 3 shows four 'diffusion curves' obtained from the four separate diffusion loss experiments. Fig. 3a is a diffusion curve from a PDMS chip without an implant and shows a fluid sample loss of nearly 1.25 μl after 35 thermal cycles (about a 75% loss of sample). Fig. 3b is a diffusion curve from a PDMS chip without an implant but with the glass capping; this shows a fluid loss of about 0.4 μl, i.e. about a 23% fluid loss. Fig. 3c and d are diffusion curves from PDMS chips that were fabricated with a PE vapour barrier implanted in the PDMS using the chemical and physical implant methods, respectively. These show a loss of about 0.4 μl, again corresponding to about a 23% sample loss.

We have observed that samples that lost more than about 50% of their volume during the PCR stage were generally unsuccessfully amplified and we attribute this to some combination of temperature non-uniformity caused by the partially filled well (partially filled chambers are known to cause a temperature drop of up to 5 °C at the denaturation temperature [37]) and the change in reagent concentrations. In this context, Fig. 3a suggests that the PCR may only be successful if the PCR is started with a sufficiently large number of sample DNA (template) molecules so as to obtain a detectable PCR product after about 20 cycles. This was corroborated by (1) performing biochip PCR successfully (described below) with many template molecules from a sample that in conventional processing gave a strong signal within 20 cycles [34] and (2) by unsuccessfully amplifying a sample that had few template molecules and that in conventional processing [38]

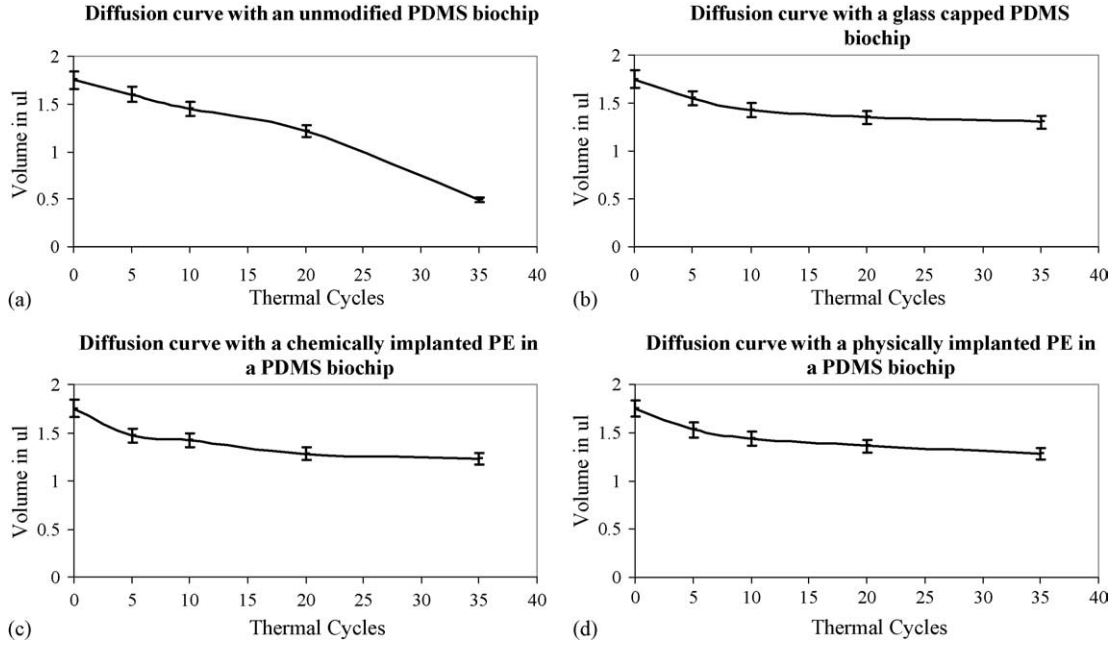

Fig. 3. Quantifying fluid sample loss resulting from PCR thermal cycling: (a) PDMS biochip without vapour barrier, (b) PDMS biochip with external glass capping, (c) PDMS biochip with vapour barrier implanted using the chemical method, (d) PDMS biochip with vapour barrier implanted using the physical method.

required at least 35 cycles to obtain a detectable signal (data not shown).

It is apparent that this loss of liquid from PDMS impairs reliable operation with microliter volumes and it is also clear that there is a need for a method of minimizing this loss lest it preclude operation with smaller volumes. While glass capping above the PCR chamber in an unimplanted biochip was a potential solution to prevent loss, it presents an additional thermal load that could cause temperature gradients in the chamber. The rigidity of the glass also hinders the operation of our pumping and valving process.

Polyethylene (PE) has very low permeation to water and water vapour—about 100 times less than that of PDMS [35] (Table 2). Due to its excellent performance as a vapour barrier, PE films are common household and food industry wrapping materials for moisture retention. PE has a melting point of 137 °C, which is well above the denaturation temperature (94 °C) in a PCR thermal cycling experiment. In addition, PE has excellent elasticity (18 MPa, ~900% at break [39]) and hence was not expected to hinder our pumping of valving methods. With such favourable properties, PE was an obvious choice as an implant material.

Diffusion curves obtained from PDMS chips with implanted PE vapour barriers (Fig. 3c and d) show much reduced fluid loss (by about a factor of 3) as compared to a PDMS chip without a vapour barrier (Fig. 3a). After 35 thermal cycles, the volume of liquid lost in an unimplanted PDMS chip was about 1.25 μl, whereas that in a PDMS chip with a PE implant it was only about 0.4 μl. There were some marginal variations in the volumes between different chips due to the slight variation in the volume of the different posts used in the fabrication process; nevertheless, all diffusion curves presented here were reproduced at least twice more than shown here, each time with similar curve patterns.

3.2. DNA fragment analysis by capillary electrophoresis

Electropherograms (relative fluorescence intensity (RFI) versus time in s) of the unimplanted on-chip PCR (Fig. 4) and the control experiment performed on the commercial thermocycler (data not shown) resulted in the same arrival times for the primer and product DNA peaks, confirming the success of our chip-based approach. The weak primer peak was seen at about 148 s and a strong product peak was seen at about 178 s. The size of the resulting product (322 base pairs) was verified by comparison with a λ*Hin*dIII–ϕX174*Hae*III size standard, as separated on a 1% agarose gel with ethidium bromide [34] (data not shown) or by the arrival time of the fluorescence peak.

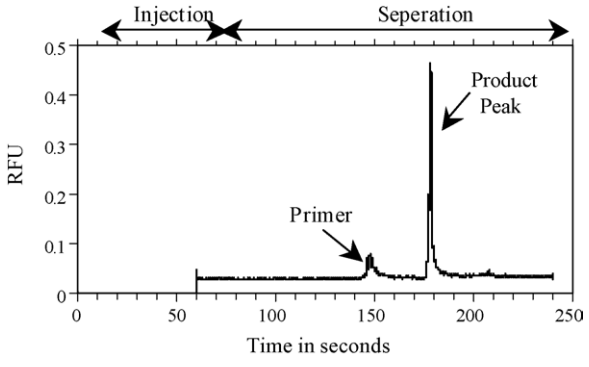

Fig. 4. On-chip PCR product analysis by capillary electrophoresis–relative fluorescence intensity vs. time in s.

The unmodified chip (i.e. no capping or implanted layer) also occasionally allowed the PCR to be successfully amplified from SCO1 samples (containing a large number of template DNA molecules) even if the retrieval was under 50% of the volume loaded; however it was invariably unable to successfully amplify samples having a small number of template molecules ([38] and Adamia et al., in preparation). On the other hand, the modified chips were able to amplify samples with either a large or small number of template molecules and could do so with a recovery of about 75% of the volume loaded. For PCR experiments in modified chips with samples having few template molecules, the yield and electropherograms were similar to those from conventional, macroscopic methods (Adamia et al., in preparation). In particular, in modified (physically implanted) chips the PCR of the SCO1 samples (large number of template molecules) gave similar product peaks to that shown in Fig. 4.

4. Discussion

4.1. Diffusion parameter estimation

PDMS is often used as a membrane material for the separation of volatile gases and vapours [21,40] but there has been little study of diffusion phenomena in PDMS under conditions of elevated temperature and pressure [28]. Such conditions are common in genetic testing applications and a better understanding of their influence will be crucial. Furthermore, diffusion parameters are known to significantly vary with different sources of PDMS [28] and hence it would be important to conduct such studies in the commonly used brands of PMDS, such as Sylgard 184. Unfortunately, to the best of our knowledge, no diffusion data are available for Sylgard 184 [28].

Experimental studies on the transport of water molecules in a few brands of PDMS (RTV 615 and PS 342.5) have been reported in the literature but large variations are apparent in the reported data, suggesting the difficult nature of predicting the behaviour of this material [22,41]. There have been controversies over the mechanisms and parameters of water movement in PDMS, but more recent measurements suggest that the diffusion coefficient of liquids and vapours in PDMS are a constant [22,41]. Watson et al. [22] have experimentally determined the diffusion coefficient of water at 25 °C to be about 2×10^{-9} m^2/s and found good agreement with theory—this value has become widely used in the literature. In the following, we apply theoretical models of the

diffusion-based losses and find that these are consistent with our experimental results.

In a diffusion process, the diffusion length d (m) is the distance a diffusing molecule can travel in a given time as given by an expression based on diffusion in an isotropic three-dimensional geometry [42]:

$$d = \sqrt{2Dt} \tag{1}$$

(d will be $\sqrt{2}$ larger for two-dimensional diffusion [43]), where D is the diffusion coefficient of water in PDMS (m^2/s) and t the time duration (s) over which the diffusion occurs. If the diffusion length and chamber size are small relative to the PDMS thickness then the diffusion process is best described by the isotropic three-dimensional case (Eq. (1)). On the other hand, in the limit of a diffusion length much larger than the PDMS thickness and chamber size, the diffusion process is best described by the two-dimensional case. Since these two cases differ by only about 40%, we use Eq. (1) for our estimates.

The diffusion coefficient is expected to exponentially vary with temperature and is described by an Arrhenius relationship [44]:

$$D = D_0\,(e^{-E_D/RT}) \tag{2}$$

where D_0 is the pre-exponential factor of diffusion coefficient, E_D the activation energy (found to be 14 kJ/mol) [22], R the gas constant (8.3 J/mol K) [45] and T the temperature in K. Within the PCR thermal cycling temperature range, the ratio of D at the maximum (94 °C) and minimum (60 °C) PCR temperatures differ by less than a factor of 2. Given the large variation (by orders of magnitude [22,28,41]) in the literature of estimates of the diffusion coefficient of water in PDMS, our estimated variation in the coefficient over the PCR temperature range is negligible. Hence, in our calculations we take the value of D for water to be a constant throughout the PCR temperature range and the total time of the experiment as being the time for which the diffusion process occurs. We take this value to be 2×10^{-9} m^2/s. Therefore, from Eq. (1), the diffusion length d for a 35-cycle PCR experiment lasting ~7000 s is estimated to be 5.5 mm.

In a simplified model of the chip without an implant, we consider the loss mechanisms to be a combination of vapour loss to the atmosphere and volumetric loss (absorption) by the bulk of the PDMS, as depicted in Fig. 5. The shortest distance the water molecules have to travel before vapour loss to the atmosphere occurs is across the 1 mm thick PDMS chamber roof. Since this distance is much less that any other distance, we expect this 'vertical' loss to be the dominant form of vapour loss in the unmodified chip. By implanting a low permeability PE layer, the overall sample loss was reduced by a factor of 3 (Fig. 3a and c) and we attribute this to a reduction in vertical vapour loss. The loss still seen in the implanted chip is due to volumetric loss (as estimated below).

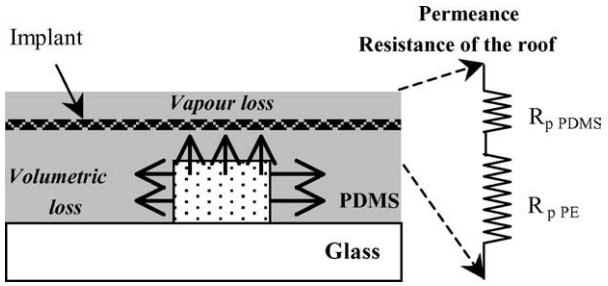

Fig. 5. (Left) A cross-section depiction of the PDMS–glass chip with a polyethylene implant. Vapour loss is expected across the 1 mm thick roof while volumetric loss is expected in the bulk PDMS along the walls of chamber. (Right) Permeance resistance modeling of the 1 mm roof of the PDMS chip with a polyethylene implant.

4.1.1. Volumetric loss

The dimensions of the bulk PDMS below the implant are 19 mm (length) × 8 mm (width) × ~1 mm (thickness). The scale of the diffusion length d (5.5 mm as calculated above) is comparable to that of the chip and we expect the water to diffuse throughout a volume of approximately $\pi R^2 H$ from the PCR chamber i.e. ~96 mm^3 where R is 5.5 mm and H is 1 mm. If we assume that Sylgard 184 will absorb the same quantity of water as RTV615 PDMS (given as 0.38% (w/w) by Blume et al. [46]), the volumetric loss by the bulk PDMS below the implant for the above estimated diffusion length would be ~0.35 μl. In our experiment in a chip with a PE vapour barrier implant, the water loss was about 0.4 μl, which is consistent with our theoretical estimation of the volumetric loss. Also, the equality of the losses from the implanted and glass-capped chips suggests that the vertical vapour loss has been eliminated. The agreement between the theoretical and experimental data suggest that the remaining loss in our modified PDMS chips was predominantly volumetric loss.

4.1.2. Vertical vapour loss

Flux is defined as the rate at which a gas or a fluid flows across the polymer (usually expressed as flow per unit area per unit time having the units of l/s m^2, g/s m^2, or mol/s m^2). The relationship between the flux (F) across a membrane and the diffusion coefficient (D) is given by

$$F = D\left(\frac{dC}{dd}\right) \tag{3}$$

where C is the concentration of water in the PDMS (l/m^3) and d the membrane thickness across which the diffusion occurs (m). We approximate our PCR well as consisting of a 1 mm membrane with a surface area of 3.14 mm^2 (i.e. the PCR chamber roof). Assuming a 0.38% (w/w) sorption value for Sylgard 184, C would be 3.8 l/m^3. Thus, with the reported diffusion coefficient value (Table 1), the flux from Eq. (3) would be 8.36 μl/s m^2. This implies that over a thermal cycling time of 7000 s, the vapour loss would be 0.18 μl. Although this value is about four times less than the experimentally observed vapour loss of ~0.85 μl (i.e. difference in loss between a chip with and without implant), this constitutes a

good agreement given the range of the diffusion constants reported in the literature, and the fact that we have neglected the diffusion from the sidewalls of the PCR chamber. We estimate that the effect of the sidewalls would double the effective area of the membrane. Using Eq. (2) to estimate the value of D at 77 °C (the middle of the PCR temperature range), we would obtain a value 2.3 times larger than the value at 25 °C (4.6×10^{-9} m^2/s). Together these could explain our factor of 4, however, all of these parameters have high uncertainties.

4.1.3. Effect of an implant

Permeability is defined as the ability of a polymer to transmit gas and/or fluid through its pores. As calculated below, an alteration in the permeability of the structure is expected by implanting a PE vapour barrier in the PDMS. The relationship between flux and permeability in a polymer membrane is defined by [35]:

$$\frac{P}{d} = \frac{F}{A\Delta p} \tag{4}$$

where P is the permeability coefficient (g cm/cm^2 s cmHg), d the thickness of the membrane (cm), F the vapour flux (g/cm^2 s), A the membrane surface area (cm^2), and Δp the pressure difference across the membrane (cmHg).

The resistance of a material to the permeation of a vapour or liquid is defined as the 'permeance resistance' (R_p) [47,48] where higher permeance resistance indicates lower diffusion loss. The permeance of a material (P/d) is inversely proportional to the permeance resistance, R_p [47], and from Eq. (4) it is defined as

$$R_p = \frac{A\Delta p}{F} = \frac{d}{P} \tag{5}$$

As Fig. 5 depicts, the effective permeance resistance of a set of layers of material is the sum of their individual permeance resistances [47] (analogous to adding electrical resistances that are in series) with the high permeance resistance of the thin PE layer added to the permeance resistance of the thicker PDMS (the permeability values are summarized in Table 2). For simplicity of calculation, the two PDMS layers (above and below the implant in the roof of the chip) have been combined to one thicker layer. Thus, the permeance resistance of the PDMS roof structure with an implant, $R_{p\,\text{implant+ PDMS}}$ can be expressed as [47]:

$$R_{p\,\text{implant+PDMS}} = \frac{d_1}{P_{\text{PDMS}}} + \frac{d_2}{P_{\text{PE}}} \tag{6}$$

where d_1 is the total thickness of the membrane PDMS material above the chamber (965 μm), P_{PDMS} the permeability of the PDMS (80.5×10^{-11} g cm/cm^2 s cmHg), d_2 the thickness of the PE implant (35 μm), and P_{PE} the permeability of the PE (0.83×10^{-11} g cm/cm^2 s cmHg). The permeance resistance $R_{p\,\text{implant + PDMS}}$ from the above equation is calculated to be 5.3×10^8 cm^2 s cmHg/g.

Similarly the permeance resistance of the PDMS material without an implant, $R_{p\,\text{PDMS}}$, is expressed as [47]:

$$R_{p\,\text{PDMS}} = \frac{d}{P_{\text{PDMS}}} \tag{7}$$

where d is the thickness of the PDMS (1000 μm) and P_{PDMS} the permeability of the PDMS. From Eq. (7) the permeance resistance $R_{p\,\text{PDMS}}$ is calculated to be 1.2×10^8 cm^2 s cmHg/g; about four times less than the permeance resistance of a PDMS structure with a thin layer of PE implant. Hence, in an implanted chip, the vapour loss is expected to be reduced by a factor of 4. The fact that our implanted chips gave similar results to that of the glass-capped chip suggests that the vapour loss was in fact reduced to a negligible level, i.e. that the remaining loss is primarily volumetric and vapour loss from the roof of the chamber has been eliminated. This suggests that the vapour barrier has been even more effective that calculated. This might be explained by the formation of a PDMS interpenetrating polymer network (IPN) [49] wherein the intermixing of polymers effectively results in a pore filling effect and a further reduction in the vapour loss.

Quake and coworkers [26] fabricated PDMS chips containing an array of PCR chambers with many fluid-filled hydraulic channels layered above them, but sample loss from the PCR chamber was not reported. We attribute this apparent absence of fluid loss to the fact that within that design the fluid within the hydraulic channels may have saturated the pores in the PDMS so that no loss occurred from the underlying PCR chambers. We suggest then that in PDMS microfluidic devices used in experiments at elevated temperatures (apart from preventing vapour loss by the techniques demonstrated here) saturation might be considered as an additional means of greatly minimizing reagent sample loss. For example, assuming that vertical vapour loss has been suppressed with an implant, this saturation mechanism could be implemented by a 'guard channel' (analogous to a guard line in electronics) that saturates the PDMS with water along the perimeter of the chip to prevent loss. Although their description of their biochip PCR is unclear in terms of factors relating to vapour loss, Yu et al. [24] do not appear to have used fluid-filled control channels that may have saturated the PDMS. It appears though, that the high density of their sub-microlitre volume PCR wells may have allowed saturation to be reached from the wells alone.

4.2. Merits of the implant

PDMS biochips with the implanted PE are handled no differently from non-implanted biochips. Special consideration was not required for PCR. No signs of separation of the fully processed PDMS devices were found after Scotch-tape tests, however the physically implanted chips without the high temperature curing step failed these tests (Section 2.1). To further examine the adhesion strength at the implanted layer, fully processed PDMS test samples with an implant were dissected

and it was found that the layered implant could not be peeled away without tearing the layers. Furthermore, we believe that the dissolved PE and PDMS interdiffused in the implanted chips, thereby creating an IPN [49].

These PE implantation methods offer numerous advantages—first, surface-coating methods with sealants, paints or epoxies are difficult to apply. We have experimented with EpoTek301-2FL (Epoxy Tech., MA, USA), NOA60 (Norland, NJ, USA), acrylics dissolved in acetone (Anachemia Science, Edmonton, Canada), paints and found all that we have tried to be non-adherent to the PDMS or to create a rigid surface on the PDMS that cracked rather than flexed when used with our pumping and valving system. With the present implant method the flexibility of the PDMS was unchanged and hence the pumping and valving remained unaffected. Second, irreversible bonding of the PDMS to a glass substrate using the O_2 plasma technique was not affected because the exterior surface chemistry of the PDMS was unaffected with this layered implantation fabrication protocol. Third, since the implanted material is not in direct contact with the PCR sample, inhibition of the PCR genetic amplification by the implant material was not a concern. Thus, this implant method provides a simple, inexpensive and straightforward approach that was readily adopted within the soft-lithography process without the requirement of special equipment. Further, this method also lends itself to multi-layer implantations.

4.3. Alternative materials for implantation

In this work we presented diffusion data from PE implanted PDMS biochips (Fig. 3c and d), although fluoropolymer (Dyneon THV220, kindly provided by 3M Inc., Ont., Canada) and poly(vinylidene chloride) (Saran®) implants also showed good vapour diffusion barrier properties and the final fluid volumes retrieved were similar to those with PE (data not shown). However, the high rigidity of the fluoropolymer (flexural modulus = 80 MPa) made the biochip incompatible with our pumping and valving system. Table 2 lists polymers with low water vapour permeability that might be used as implants or copolymer fillers in the PDMS to counteract vapour diffusion. Suggested solvents for the polymers [30] with their experimental swelling ratios (defined as the ratio of the length of the polymer in the solvent to the length of the dry polymer) [31] in PDMS are also summarized in Table 2. Choosing a solvent that is only partially absorbed by the PDMS is critical in successfully performing this implantation protocol in a controlled manner as highly absorbing solvents may cause extensive swelling and deformation of the chip features in the PDMS [31].

5. Conclusion

Water loss in PDMS microfluidic devices has limited their use in applications with small volumes at elevated temperatures. To our knowledge, the only reports of PDMS-based sub-microlitre PCR are from work that has been performed with high-density arrays of PCR wells and these compact geometries may have enabled their success [24,26]. However, with higher levels of integration (e.g. incorporating CE) this density may be lost, possibly preventing the operation of small scale PCR in integrated devices. Obviously, a means of better controlling this vapour loss is needed. In this work we have explored the loss mechanisms and their control, and demonstrated small volume PCR genetic amplification in PDMS biochips. We showed that the loss during the PCR thermal cycling was primarily due to vapour loss from the chip. We have demonstrated a new method for microfabricating PDMS devices with an implanted PE vapour barrier. This barrier substantially reduced the vapour diffusion (and hence reduced the water loss) from the PDMS biochip when the PCR was performed. This method is an inexpensive and straightforward approach that is accomplished without the requirement of unusual equipment. With these modifications we were able to successfully perform the PCR with samples that could not be successfully amplified on unmodified chips (Adamia et al., in preparation).

Our experimental observations indicate that the vapour loss from the roof of the chip was prevented by the implanted layer. In an implanted chip, the observed small fluid loss is attributed to volumetric loss (i.e. loss through the sidewalls) and this was consistent with a theoretical estimate. The volumetric loss can be reduced by limiting the volume of PDMS that is available for absorbing water or by using ‘guard channels’. This finding is hoped to enable smaller volume PCR in future PDMS developments.

Integrated diaphragm pumping and pinch-off valving provided a robust fluidic control system suitable for PCR genetic amplification and is capable of repeated cycles of sample loading and unloading in an automated fashion. Work is ongoing in optimizing and building integrated PDMS devices that will be capable of small volume PCR genetic amplification and PCR product detection with automated and fully reusable robust valves and pumps.

Acknowledgements

We gratefully acknowledge the support of the Natural Sciences and Engineering Research Council (NSERC) of Canada for this research. The authors would also like to thank Loi Hua for technical assistance with electronics, D. Moira Glerum for biological sample resources, Elizabeth Dickinson, Jana Lauzon and Alex Stickel for laboratory assistance.

References

[1] C.H. Mastrangelo, M.A. Burns, D.T. Burke, Microfabricated devices for genetic diagnostics, Proc. IEEE 86 (1998) 1769–1787.
[2] J. Wang, Microchip devices for detecting terrorist weapons, Anal. Chim. Acta 507 (2004) 3–10.

[3] D. Erickson, D. Li, Integrated microfluidic devices, Anal. Chim. Acta 507 (2004) 11–26.
[4] P.J. Obeid, T.K. Christopoulos, H.J. Crabtree, C.J. Backhouse, Microfabricated device for DNA and RNA amplification by continuous-flow polymerase chain reaction and reverse transcription-polymerase chain reaction with cycle number selection, Anal. Chem. 75 (2003) 288–295.
[5] L.J. Kricka, P. Wilding, Microchip PCR, Anal. Bioanal. Chem. 377 (2003) 820–825.
[6] E.T. Lagally, P.C. Simpson, R.A. Mathies, Monolithic integrated microfluidic DNA amplification and capillary electrophoresis analysis system, Sens. Actuators B: Chem. 63 (2000) 138–146.
[7] H. Nagai, Y. Murakami, Y. Morita, K. Yokoyama, E. Tamiya, Development of a microchamber array for picoliter PCR, Anal. Chem. 73 (2001) 1043–1047.
[8] J.N. Yang, Y.J. Liu, C.B. Rauch, R.L. Stevens, R.H. Liu, R. Lenigk, P. Grodzinski, High sensitivity PCR assay in plastic micro reactors, Lab on a Chip 2 (2002) 179–187.
[9] B.C. Giordano, J. Ferrance, S. Swedberg, A.F.R. Huhmer, J.P. Landers, Polymerase chain reaction in polymeric microchips: DNA amplification in less than 240 s, Anal. Biochem. 291 (2001) 124–132.
[10] P. Sethu, C.H. Mastrangelo, Cast epoxy-based microfluidic systems and their application in biotechnology, Sens. Actuators B: Chem. 98 (2004) 337–346.
[11] J.W. Hong, T. Fujii, M. Seki, T. Yamamoto, I. Endo, Integration of gene amplification and capillary gel electrophoresis on a polydimethylsiloxane–glass hybrid microchip, Electrophoresis 22 (2001) 328–333.
[12] J.C. McDonald, G.M. Whitesides, Poly(dimethylsiloxane) as a material for fabricating microfluidic devices, Acc. Chem. Res. 35 (2002) 491–499.
[13] B.D. Gates, G.M. Whitesides, Replication of vertical features smaller than 2 nm by soft lithography, J. Am. Chem. Soc. 125 (2003) 14986–14987.
[14] J.C. Lotters, W. Olthuis, P.H. Veltink, P. Bergveld, The mechanical properties of the rubber elastic polymer polydimethylsiloxane for sensor applications, J. Micromech. Microeng. 7 (1997) 145–147.
[15] J. Kim, M.K. Chaudhury, M.J. Owen, Hydrophobicity loss and recovery of silicone HV insulation, IEEE Trans. Dielectr. Electr. Insul. 6 (1999) 695–702.
[16] H. Hillborg, U.W. Gedde, Hydrophobicity changes in silicone rubbers, IEEE Trans. Dielectr. Electr. Insul. 6 (1999) 703–717.
[17] J.C. Lotters, W. Olthuis, P.H. Veltink, P. Bergveld, Polydimethylsiloxane, a photocurable rubberelastic polymer used as spring material in micromechanical sensors, Microsyst. Technol. 3 (1997) 64–67.
[18] N.L. Jeon, D.T. Chiu, C.J. Wargo, H.K. Wu, I.S. Choi, J.R. Anderson, G.M. Whitesides, Design and fabrication of integrated passive valves and pumps for flexible polymer 3-dimensional microfluidic systems, Biomed. Microdev. 4 (2002) 117–121.
[19] W.H. Grover, A.M. Skelley, C.N. Liu, E.T. Lagally, R.A. Mathies, Monolithic membrane valves and diaphragm pumps for practical large-scale integration into glass microfluidic devices, Sens. Actuators B: Chem. 89 (2003) 315–323.
[20] M.A. Unger, H.-P. Chou, T. Thorsen, A. Scherer, S.R. Quake, Monolithic microfabricated valves and pumps by multilayer soft lithography, Science 288 (2000) 113–116.
[21] T.C. Merkel, V.I. Bondar, K. Nagai, B.D. Freeman, I. Pinnau, Gas sorption, diffusion, and permeation in poly(dimethylsiloxane), J. Polym. Sci. Part B: Polym. Phys. 38 (2000) 415–434.
[22] J.M. Watson, M.G. Baron, The behaviour of water in poly(dimethylsiloxane), J. Membrane Sci. 110 (1996) 47–57.
[23] Y.S. Shin, K. Cho, S.H. Lim, S. Chung, S.J. Park, C. Chung, D.C. Han, J.K. Chang, PDMS-based micro PCR chip with parylene coating, J. Micromech. Microeng. 13 (2003) 768–774.
[24] X.M. Yu, D.C. Zhang, T. Li, L. Hao, X.H. Li, 3-D microarrays biochip for DNA amplification in polydimethylsiloxane (PDMS) elastomer, Sens. Actuators A: Phys. 108 (2003) 103–107.
[25] J. Liu, M. Enzelberger, S. Quake, A nanoliter rotary device for polymerase chain reaction, Electrophoresis 23 (2002) 1531–1536.
[26] J. Liu, C. Hansen, S.R. Quake, Solving the "world-to-chip" interface problem with a microfluidic matrix, Anal. Chem. 75 (2003) 4718–4723.
[27] J.M.K. Ng, I. Gitlin, A.D. Stroock, G.M. Whitesides, Components for integrated poly(dimethylsiloxane) microfluidic systems, Electrophoresis 23 (2002) 3461–3473.
[28] W.J. Chang, D. Akin, M. Sedlak, M.R. Ladisch, R. Bashir, Poly(dimethylsiloxane) (PDMS) and silicon hybrid biochip for bacterial culture, Biomed. Microdev. 5 (2003) 281–290.
[29] C.R. Tamanaha, L.J. Whitman, R.J. Colton, Hybrid macro–micro fluidics system for a chip-based biosensor, J. Micromech. Microeng. 12 (2002) N7–N17.
[30] J. Brandrup, E. Immergut, Polym. Handbook, third ed., Wiley Interscience, NY, USA, 1989, pp. iv-185–iv-234.
[31] J.N. Lee, C. Park, G.M. Whitesides, Solvent compatibility of poly(dimethylsiloxane)-based microfluidic devices, Anal. Chem. 75 (2003) 6544–6554.
[32] H. Andersson, W. van der Wijngaart, P. Nilsson, P. Enoksson, G. Stemme, A valve-less diffuser micropump for microfluidic analytical systems, Sens. Actuators B: Chem. 72 (2001) 259–265.
[33] I. Erill, S. Campoy, N. Erill, J. Barbe, J. Aguilo, Biochemical analysis and optimization of inhibition and adsorption phenomena in glass-silicon PCR-chips, Sens. Actuators B: Chem. 96 (2003) 685–692.
[34] C.J. Backhouse, H.J. Crabtree, D.M. Glerum, Frontal analysis on a microchip, Analyst 127 (2002) 1169–1175.
[35] J.R. Fried, Polymer Science and Technology, second ed., Prentice Hall Professional Technical Reference, NJ, USA, 486–533.
[36] H.J. Crabtree, E.C.S. Cheong, D.A. Tilroe, C.J. Backhouse, Microchip injection and separation anomalies due to pressure effects, Anal. Chem. 73 (2001) 4079–4086.
[37] D.S. Yoon, Y.S. Lee, Y. Lee, H.J. Cho, S.W. Sung, K.W. Oh, J. Cha, G. Lim, Precise temperature control and rapid thermal cycling in a micromachined DNA polymerase chain reaction chip, J. Micromech. Microeng. 12 (2002) 813–823.
[38] S. Adamia, T. Reiman, M. Crainie, A. Belch, L. Pilarski, Aberrant splicing of hyaluronan synthase 1 (HAS1) gene in multiple myeloma (MM): HAS1 and novel HAS1 variants in MM b cells have an adverse impact on patient survival, Blood 102 (2003) 371.
[39] A.E. Goulas, K.A. Riganakos, A. Badeka, M.G. Kontominas, Effect of ionizing radiation on the physicochemical and mechanical properties of commercial monolayer flexible plastics packaging materials, Food Addit. Contam. 19 (2002) 1190–1199.
[40] C.K. Yeom, S.H. Lee, H.Y. Song, J.M. Lee, Vapor permeations of a series of VOCs/N-2 mixtures through PDMS membrane, J. Membrane Sci. 198 (2002) 129–143.
[41] M.E. Rezac, T. John, P.H. Pfromm, Effect of copolymer composition on the solubility and diffusivity of water and methanol in a series of polyether amides, J. Appl. Polym. Sci. 65 (1997) 1983–1993.
[42] K. Pappaert, J. Vanderhoeven, P. Van Hummelen, B. Dutta, D. Clicq, G.V. Baron, G. Desmet, Enhancement of DNA micro-array analysis using a shear-driven micro-channel flow system, J. Chromatogr. A 1014 (2003) 1–9.
[43] K.S. McCain, D.C. Hanley, J.M. Harris, Single-molecule fluorescence trajectories for investigating molecular transport in thin silica sol–gel films, Anal. Chem. 75 (2003) 4351–4359.
[44] S.C. George, S. Thomas, Transport phenomena through polymeric systems, Prog. Polym. Sci. 26 (2001) 985–1017.
[45] R. Weast, Handbook of Chemistry and Physics, CRC Press, Ohio, 1973–1974.
[46] I. Blume, P.J.F. Schwering, M.H.V. Mulder, C.A. Smolders, Vapor sorption and permeation properties of poly(dimethylsiloxane) films, J. Membrane Sci. 61 (1991) 85–97.

[47] F. Peng, J. Liu, J. Li, Analysis of the gas transport performance through PDMS/PS composite membranes using the resistances-in-series model, J. Membrane Sci. 222 (2003) 225–234.
[48] J.M.S. Henis, M.K. Tripodi, Composite hollow fiber membranes for gas separation—the resistance model approach, J. Membrane Sci. 8 (1981) 233–246.
[49] J.S. Turner, Y.L. Cheng, Preparation of PDMS–PMAA interpenetrating polymer network membranes using the monomer immersion method, Macromolecules 33 (2000) 3714–3718.
[50] D. Armani, C. Liu, N. Aluru, Proceedings of the 12th IEEE International Conference on Micro Electro Mechanical Systems MEMS'99, 1999, pp. 222–227.

Biographies

A. Ranjit Prakash received his Bachelor of Engineering degree in instrumentation and control engineering from the University of Madras, India, in 2001 and a Master of Science in electrical and computer engineering in 2004 from the University of Alberta, Canada, with focus on bioMEMS fabrication, instrumentation, and thermal control schemes for performing genetic analysis. Presently, he works at the University of Calgary, Canada in the development of integrated bioMEMS devices for genetic analysis.

S. Adamia is a Ph.D. student (supervisor Linda M. Pilarski) at the University of Alberta, Faculty of Medicine and Dentistry, Department of Oncology and a visiting researcher at the National Institute of Nanotechnology (NINT-NRC). Previous degrees and qualifications: UNSCO student—International Training Course on Topics of Modern Biology, Biological Research Center, Hungarian Academy of Sciences, Neurobiology, Department of Biochemistry (Sponsors: International Cell Research Organization, UNESCO). Honours Diploma (equivalent to M.Sc.)—Biology Faculty, Georgian State University, Tbilisi, USSR. Specialization—Biophysics; Qualifications—Biophysicist and teacher of Biology and Chemistry.

V. Sieben received his B.Sc. in Electrical Engineering from the University of Alberta, Canada in 2003. He is currently pursuing graduate studies under the supervision of Dr. Chris Backhouse at the University of Alberta with his primary research focus towards the application of DNA self-assembly for utilization in nano-scale fabrication.

P. Pilarski received his B.Sc. in Electrical Engineering from the University of British Columbia, Canada in 2003. He is currently pursuing graduate studies under the supervision of Dr. Chris Backhouse at the University of Alberta with a research focus upon the application of genetic algorithms to nanostructural characterization.

L.M. Pilarski obtained her Ph.D. from the University of Adelaide in South Australia and did postdoctoral work in immunology at the John Curtin School of Medical Research, Australian National University in Canberra. She is Canada Research Chair in Biomedical Nanotechnology, Professor of Oncology at the University of Alberta, and Senior Scientist of the Alberta Cancer Board. Her research focuses on blood cancers, molecular biology and cancer profiling on microfluidics platforms.

C.J. Backhouse graduated from the University of Alberta with a B.Sc. (1985, Physics), and the University of British Columbia with a M.Sc. (1987, Physics/Radio Astronomy) and Ph.D. (1992, Electrical Engineering). He is presently a Professor in the Electrical Engineering Department at the University of Alberta with research interests in miniaturized systems, particularly for application in the life sciences.